Supporting Information

Rapid, at-sea detection of munition compounds in seawater using a shipboard system

Mario Esposito[1*], Aaron J. Beck[1], Maria Martinez-Cabanas[1,2], Martha Gledhill[1], Eric P. Achterberg[1]

[1]GEOMAR Helmholtz Centre for Ocean Research Kiel, Wischhofstraße 1-3, 24148 Kiel, Germany

[2]Departamento de Química and CICA - Centro Interdisciplinar de Química e Bioloxía. Universidade da Coruña, 15008 A Coruña, Spain

*Correspondence to Mario Esposito, email:mesposito@geomar.de

Table of Contents

Table S1. Sorbents used for optimisation of extraction of explosives from aqueous samples.

Sorbent name	Brand	Material	Particle and Pore size	References
EASY	Chromabond	Polar polystyrene divinylbenzene with a weak anion exchanger (WAX)	80 µm, 50 Å	[1]
ENV	Bond Elut	Polystyrene-Divinylbenzene polymer	125 µm, 450 Å	[2]
HLB	Waters Oasis	Hydrophilic modified styrene polymer	50-70 µm, 80 Å	[3–5]
HR-XAW	Chromabond	Hydrophobic polystyrene divinylbenzene with secondary and tertiary ammonium modification, weak mixed-mode anion exchanger (WAX)	85 µm, 55–65 Å	not yet reported for extraction of explosives
HR-X	Chromabond	Hydrophobic polystyrene divinylbenzene copolymer	45 µm, 55–60 Å	not yet reported for extraction of explosives
Porapak R	Supelco	vinylpyrrolidone	150 µm, na	[6,7]
Porapak RDX	Sep-Pak Waters	Polydivinylbenzene-vinylpyrrolidone	125-150 µm, 200 Å	[2,8–10]

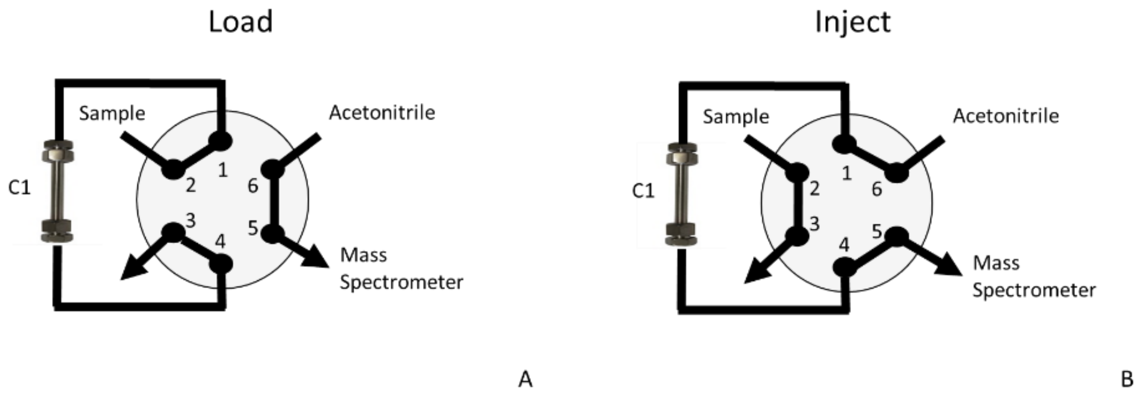

Figure S1. Continuous flow setup for extraction and elution of munition compounds from water samples. (A) The sample is pumped over one column (C1) packed with resin using an HPLC pump to extract munition compounds. (B) Analytes adsorbed on the resin are eluted from C1 with acetonitrile and directed to the mass spectrometer using a second HPLC pump by switching the 6-port valve to the “inject” position.

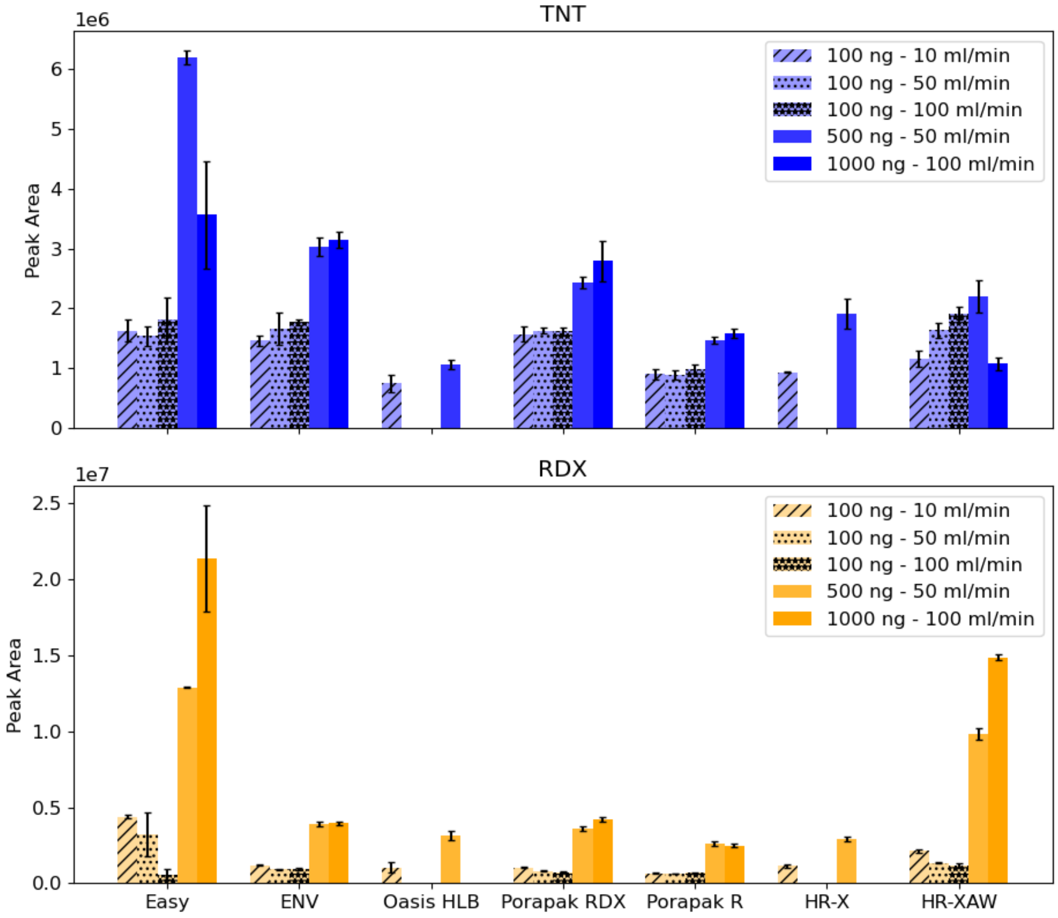

Figure S2. Comparison of extraction efficiency of TNT and RDX loaded on 7 different resins at variable flow rates and concentrations. Error bars represent the standard deviation of 3 replicates.

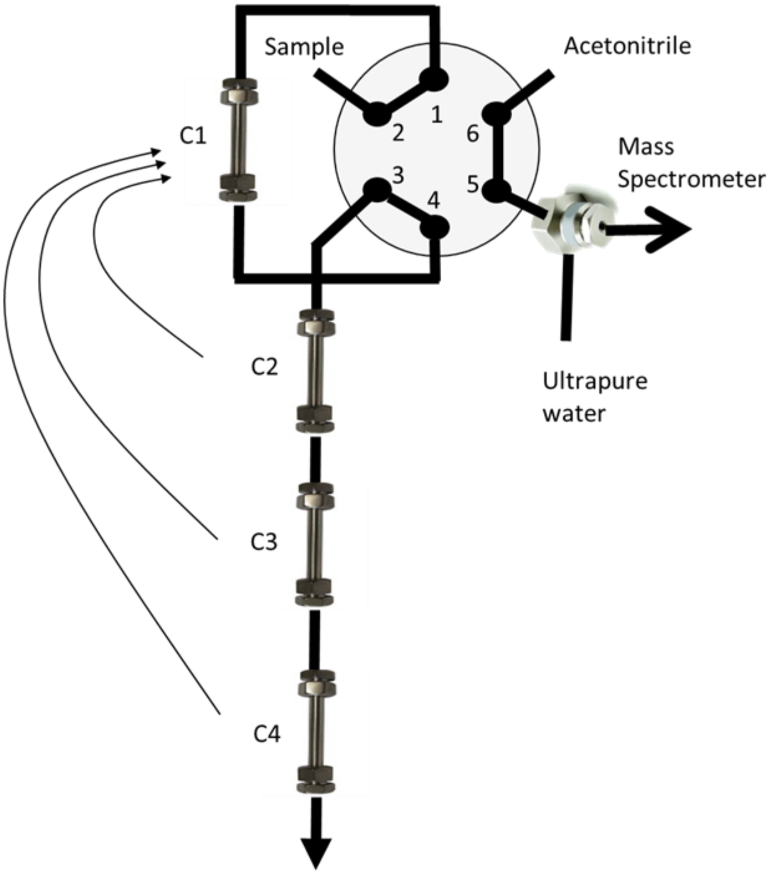

Figure S3. Schematics of the valve and columns configuration used to test resins extraction capacity. Columns: C1 to C3, size 10 x 2.1 mm I.D. and C4, size 50 x 2.1 mm I.D.

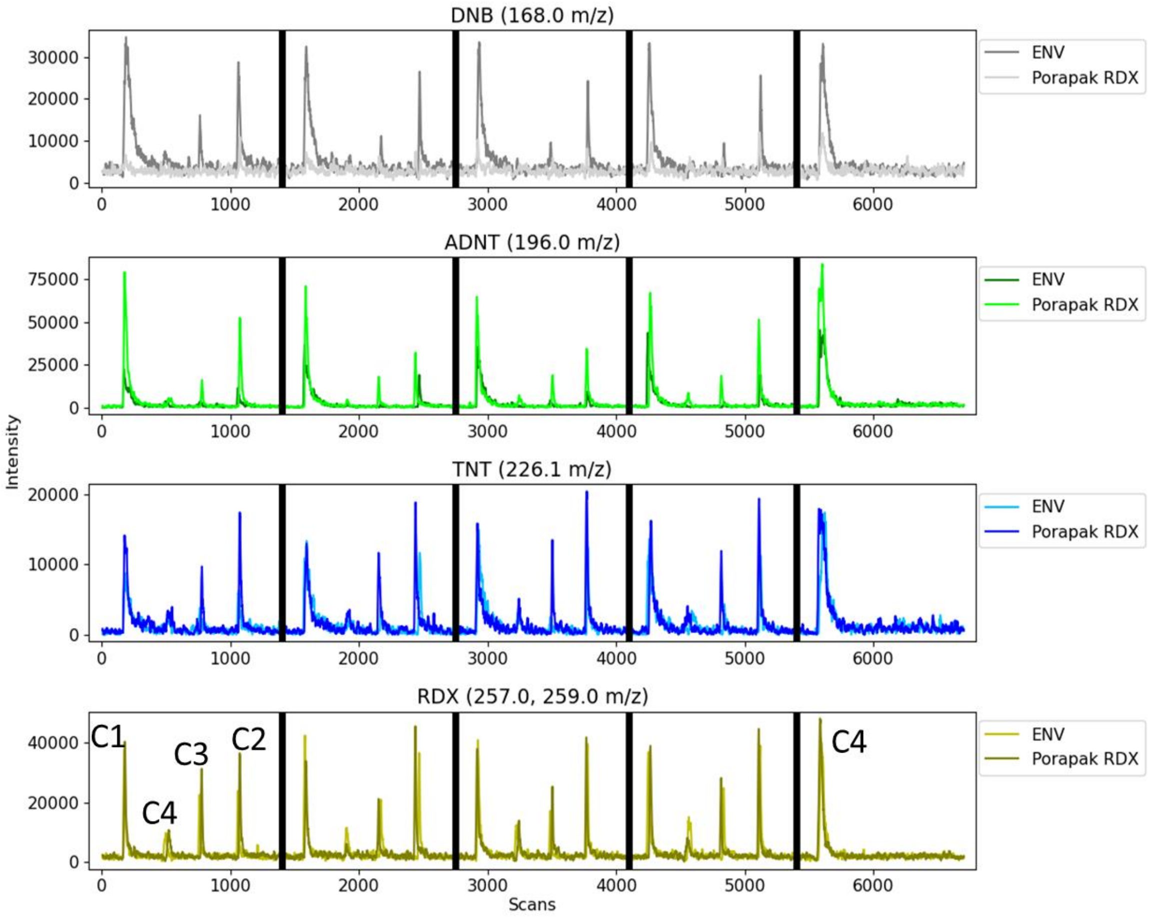

Figure S4. Mass spectrometer analysis scans of munition compounds (DNB, ADNT, TNT and RDX) loaded on and eluted from Bond Elut ENV and Porapak RDX resins packed into 4 columns (C1 to C3, size 10 x 2.1 mm I.D. and C4 size, 50 x 2.1 mm I.D.). The scans from the two resins are overlapped for graphical purposes.

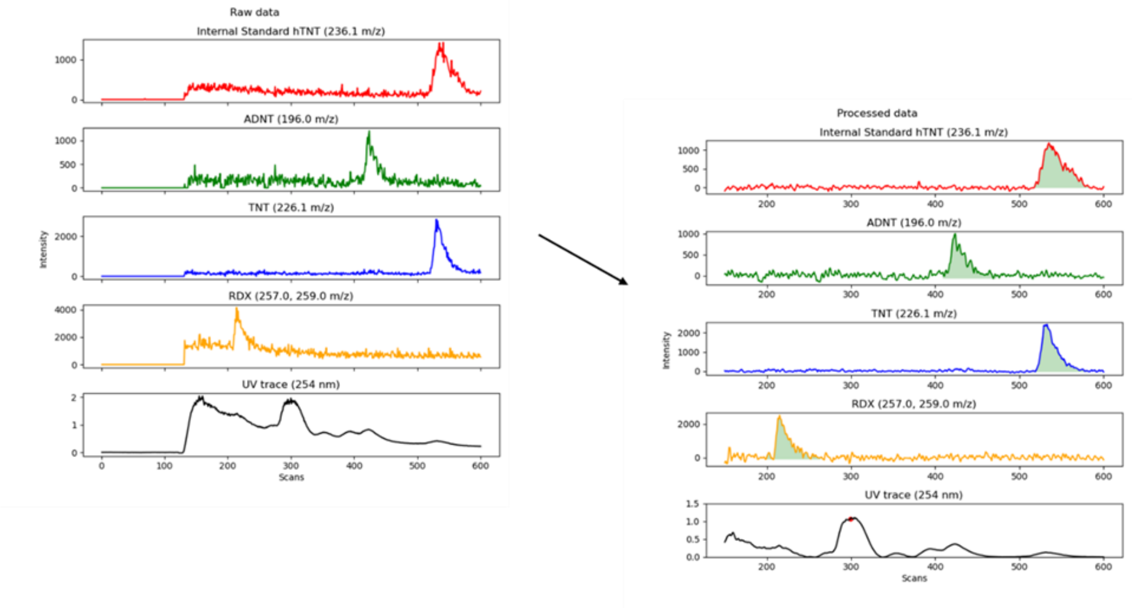

Figure S5. Processing procedure for MS and UV data. Chromatogram of 50 ng of mixed munition compounds (RDX, DNB, ADNT, hTNT and TNT) diluted in 500 ml of natural seawater from Kiel fjord (Germany).

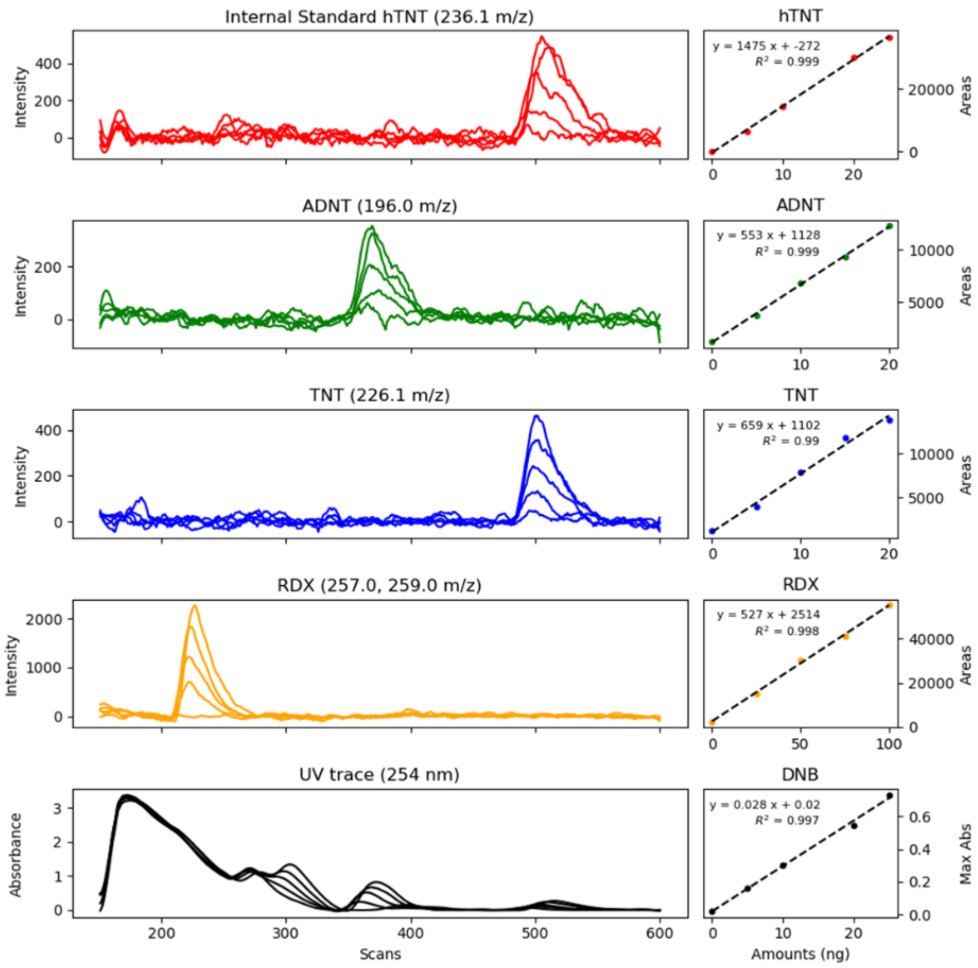

Figure S6. Calibration runs (overlapped) and regression lines of munition compounds (hTNT, ADNT, TNT, RDX and DNB) determined by MS spectrometry and UV detection (DNB only).

Determination of optimal HPLC columns and conditions

In the current work, HPLC columns were tested based on literature reports (Table S2). The HPLC column in the Gledhill method [11] has a small diameter and pore size, resulting in high backpressures that exceed the ExPloTect system capabilities. As a result, the column test list was limited to columns operating at typical HPLC conditions (<400 bar, non-UHPLC). All columns except the Diol column are reverse-phase, whereas the Diol column is normal-phase. The Diol column was tested to evaluate if normal-phase separation would be preferable given the preceding SPE conditions.

Table S2. HPLC column specifications reported in the literature for separation of nitroaromatic and nitramine explosives.

Column type	Dimensions	Particle size	Reference
C18	250 x 4.6 mm	5 µm	12
	150 x 4.6 mm	5 µm	13
	Various	5 µm	14
	150 x 4 mm	5 µm	15
	150 x 2.1 mm	3 µm	16
	250 x 4.6 mm	5 µm	17
C8	150 x 3.9 mm	n.r.	18
			19
	150 x 4 mm	5 µm	15
CN	250 x 4.6 mm	5 µm	12
	Various	5 µm	14
	250 x 4.6 mm	5 µm	17
Diol	150 x 4.6 mm	3 µm	13

n.r.: not reported

The performance of the four chosen columns was tested using a biocompatible ultra-high performance liquid chromatographic system (UHPLC, Ultimate 3000, ThermoFisher) consisting of dual high pressure pumps, a column oven, and an ultraviolet (UV) -visible diode array detector. A high resolution quadrapole/Orbitrap mass spectrometer (HESI-MS, Q Exactive, ThermoFisher) was used for detection. The UHPLC-HESI-MS was controlled with Xcalibur and Chromeleon software.

Tests focused on an isocratic method using acetonitrile (ACN) instead of MeOH to match the effluent of the SPE module. Separation of the target analytes (mixed analytical standard; EPA 8330b, Restek, Germany) was tested by varying the concentration of the ACN mobile phase and the column temperature. Chromatograms were obtained for separation of the target munition compounds, TNT (trinitrotoluene), ADNT (2- and 4- amino-dinitrotoluene), RDX (Royal Demolition Explosive), and DNB (dinitrobenzene). Mobile phase solvent concentration and column temperature control the speed at which the various analyte peaks travel through the column. The objective was to identify a column that provides excellent peak separation within the target time (10 min).

To test the required mass resolution for detection of the target compounds, a sample of Baltic Sea water was spiked with the target compounds and preconcentrated using the ExPloTect SPE method. This provided a matrix-matched sample containing the natural organic matter that can interfere with MS detection. This sample was analyzed according to the developed HPLC method, with detection on the high mass resolution Orbitrap mass spectrometer. The mass resolution was varied virtually in the Xcalibur software to test the effect on detection of the target compound and interference by non-target natural organic matter.

HPLC column separation of target analytes

Chromatograms for the C18, C8, and CN columns are shown in Figs. S7-S9. Initial tests with the Diol column gave unsatisfactory results, and further testing of that column was abandoned. For all the columns, increasing ACN concentration and temperature increased the elution time on the column. For brevity, only the ACN concentration effect is shown here. This effect was most marked for C18, which showed a decrease in elution time from 23 minutes at 30% ACN to less than 8 minutes at 60% ACN (Figure S7).

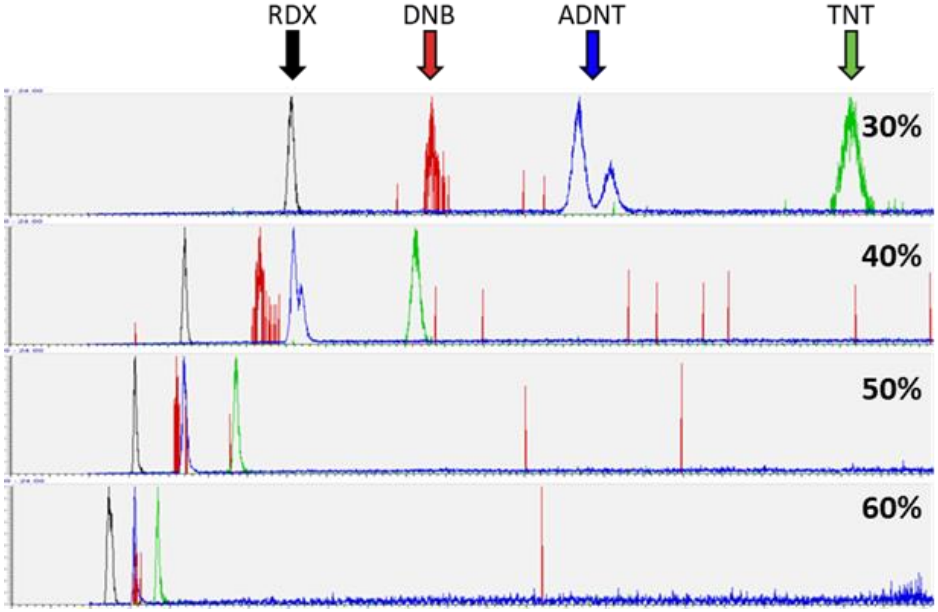

Figure S7. Chromatograms for the C18 column. Peak intensities are normalized to minimize sensitivity differences. Time on the abcissa covers approximately 25 minutes. RDX is shown in black, DNB in red, ADNT in blue, and TNT in green. Increasing ACN concentration is shown in panels from top to bottom: 30, 40, 50, and 60% ACN.

In contrast, the CN column showed target compound elution in less than 15 min for all tested concentrations (Figure S9).

At the 30% ACN concentration, the C18 and C8 columns showed separation of the two ADNT isomers, but this was markedly reduced in the C18 column at 40% ACN compared with the C8 column. The CN column showed no separation of the two isomers at any of the tested concentrations.

Although the CN column showed the fastest overall elution times, peak separation was poor. The target analytes eluted only in the second half of the chromatography, and increasing temperature and ACN concentration resulted in poor peak separation (Figure S9). Thus, the CN column was judged inappropriate for meeting the target chromatography duration.

The C18 column showed excellent separation at the lowest ACN concentration, but very slow elution (Figure S7). To meet the target chromatography time, higher ACN concentrations would be required but would result in poor peak separation.

The C8 column showed the best balance of peak separation and speed (Figure S8). At approximately 40% ACN, all target compounds eluted within 10 minutes, with sharp peaks and good separation of even the ADNT isomers. The C8 column was therefore chosen as the best option for the ExPloTect system.

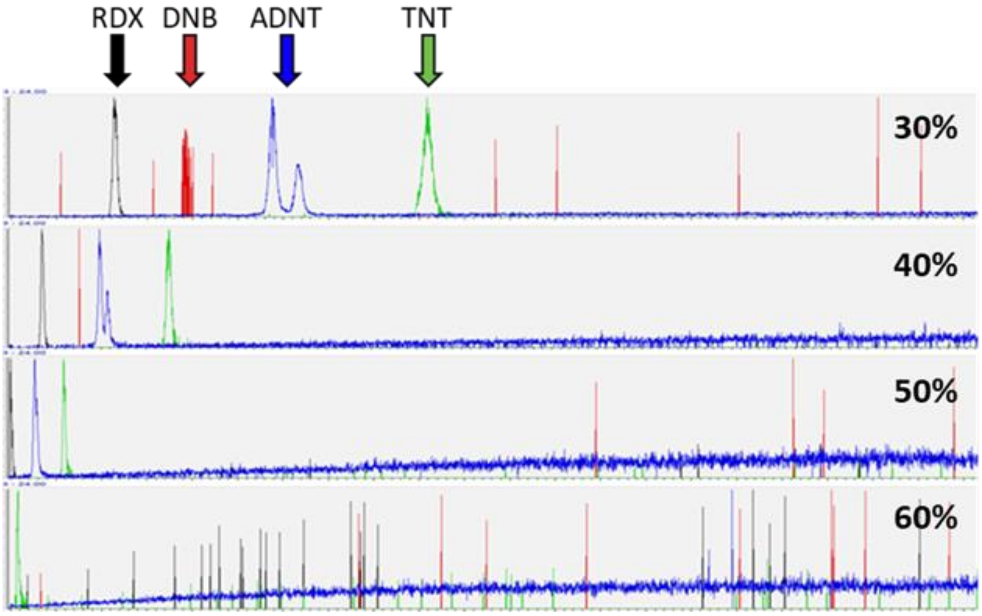

Figure S8. Chromatograms for the C8 column. Symbols as in Fig. S7

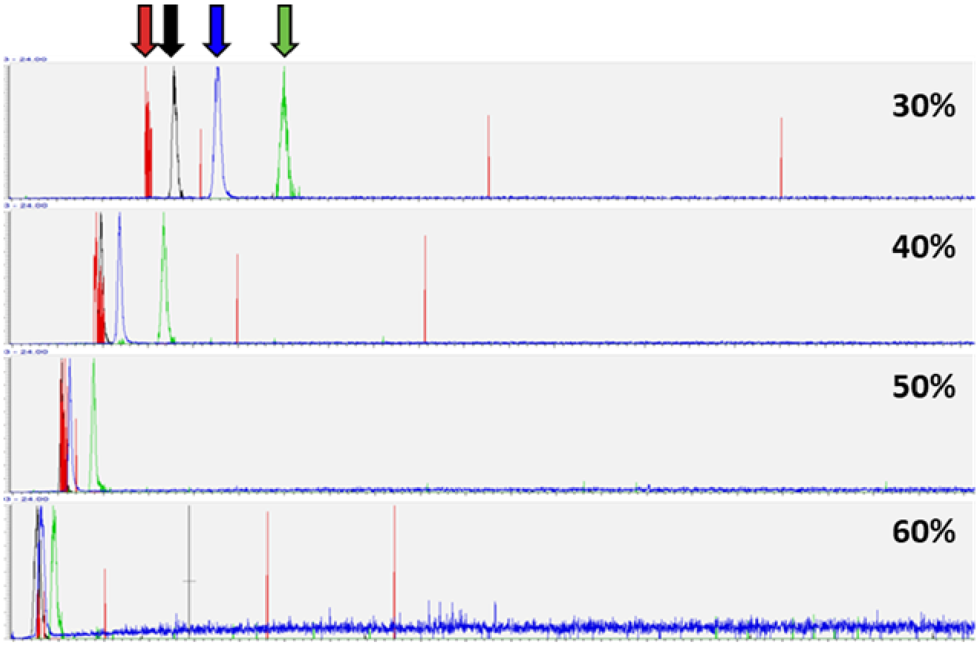

Figure S9. Chromatograms for the CN column. Symbols as in Fig. S7.

Reference list

(1) Gledhill, M.; Beck, A. J.; Stamer, B.; Schlosser, C.; Achterberg, E. P. Quantification of Munition Compounds in the Marine Environment by Solid Phase Extraction – Ultra High Performance Liquid Chromatography with Detection by Electrospray Ionisation – Mass Spectrometry. *Talanta* **2019**, *200*, 366–372. https://doi.org/10.1016/j.talanta.2019.03.050.

(2) Jönsson, S.; Gustavsson, L.; van Bavel, B. Analysis of Nitroaromatic Compounds in Complex Samples Using Solid-Phase Microextraction and Isotope Dilution Quantification Gas Chromatography-Electron-Capture Negative Ionisation Mass Spectrometry. *J. Chromatogr. A* **2007**, *1164* (1–2), 65–73. https://doi.org/10.1016/j.chroma.2007.07.023.

(3) Belden, J. B.; Lotufo, G. R.; Biedenbach, J. M.; Sieve, K. K.; Rosen, G. Application of POCIS for Exposure Assessment of Munitions Constituents during Constant and Fluctuating Exposure. *Environ. Toxicol. Chem.* **2015**, *34* (5), 959–967. https://doi.org/10.1002/etc.2836.

(4) Lotufo, G. R.; George, R. D.; Belden, J. B.; Woodley, C. M.; Smith, D. L.; Rosen, G. Investigation of Polar Organic Chemical Integrative Sampler (POCIS) Flow Rate Dependence for Munition Constituents in Underwater Environments. *Environ. Monit. Assess.* **2018**, *190* (3). https://doi.org/10.1007/s10661-018-6558-x.

(5) Craig, H. D.; Jenkins, T. F.; Johnson, M. T.; Walker, D. M.; Dobb, D. E.; Pepich, B. V. Method Development and Laboratory Intercomparison of an RP-HPLC-UV Method for Energetic Chemicals in Marine Tissues. *Talanta* **2019**, *198*, 284–294. https://doi.org/10.1016/j.talanta.2019.02.005.

(6) Maskarinec, M. P.; Manning, D. L.; Harvey, R. W.; Griest, W. H.; Tomkins, B. A. DETERMINATION OF MUNITIONS COMPONENTS IN WATER BY RESIN ADSORPTION AND HIGH-PERFORMANCE LIQUID CHROMA-TOGRAPHY-ELECTROCHEMICAL DETECTION*; 1984; Vol. 302.

(7) Lee, C. K. M.; Stenstrom, M. K. Competitive Adsorption of Cyclotrimethylenetrinitramine (RDX) and Cyclotetramethylenetetranitramine (HMX); 1996; Vol. 26.

(8) Jenkins, T. F.; Thorne, P. G.; Mccormick, E. F.; Myers, K. F. Preservation of Water Samples Containing Nitroaromatics and Nitramines. *US Army Corps Eng.* **1995**, No. Special Report 95-16.

(9) Wijker, R. S.; Bolotin, J.; Nishino, S. F.; Spain, J. C.; Hofstetter, T. B. Using Compound-Specific Isotope Analysis to Assess Biodegradation of Nitroaromatic Explosives in the Subsurface. *Environ. Sci. Technol.* **2013**, *47* (13), 6872–6883. https://doi.org/10.1021/es3051845.

(10) Mariussen, E.; Stornes, S. M.; Bøifot, K. O.; Rosseland, B. O.; Salbu, B.; Heier, L. S. Uptake and Effects of 2, 4, 6 - Trinitrotoluene (TNT) in Juvenile Atlantic Salmon (Salmo Salar). *Aquat. Toxicol.* **2018**, *194*, 176–184. https://doi.org/10.1016/j.aquatox.2017.11.016.

(11) Gledhill, M.; Beck, A. J.; Stamer, B.; Schlosser, C.; Achterberg, E. P. Quantification of Munition Compounds in the Marine Environment by Solid Phase Extraction – Ultra High Performance Liquid Chromatography with Detection by Electrospray Ionisation – Mass

Spectrometry. *Talanta* **2019**, *200* (March), 366–372. https://doi.org/10.1016/j.talanta.2019.03.050.

(12) Environmental Protection Agency, U. EPA Method 8330B (SW-846): Nitroaromatics and Nitramines by High Performance Liquid Chromatography (HPLC); 1995.

(13) Gumuscu, B.; Erdogan, Z.; Guler, M. O.; Tekinay, T. Highly Sensitive Determination of 2,4,6-Trinitrotoluene and Related Byproducts Using a Diol Functionalized Column for High Performance Liquid Chromatography. *PLoS One* **2014**, *9* (6), e99230. https://doi.org/10.1371/journal.pone.0099230.

(14) Lang, M. J.; Burns, S. E. Improvement of EPA Method 8330: Complete Separation Using a Two-Phase Approach. *J. Chromatogr. A* **1999**, *849* (2), 381–388. https://doi.org/10.1016/S0021-9673(99)00591-9.

(15) Haderlein, S. B.; Weissmahr, K. W.; Schwarzenbach, R. P. Specific Adsorption of Nitroaromatic Explosives and Pesticides to Clay Minerals. *Environ. Sci. Technol.* **1996**, *30* (2), 612–622. https://doi.org/10.1021/es9503701.

(16) Rapp-Wright, H.; McEneff, G.; Murphy, B.; Gamble, S.; Morgan, R.; Beardah, M.; Barron, L. Suspect Screening and Quantification of Trace Organic Explosives in Wastewater Using Solid Phase Extraction and Liquid Chromatography-High Resolution Accurate Mass Spectrometry. *J. Hazard. Mater.* **2017**, *329*, 11–21. https://doi.org/10.1016/j.jhazmat.2017.01.008.

(17) Larson, S. L.; Martin, W. A.; Escalon, B. L.; Thompson, M. Dissolution, Sorption, and Kinetics Involved in Systems Containing Explosives, Water, and Soil. *Environ. Sci. Technol.* **2008**, *42* (3), 786–792. https://doi.org/10.1021/es0717360.

(18) Douglas, T. A.; Johnson, L.; Walsh, M.; Collins, C. A Time Series Investigation of the Stability of Nitramine and Nitroaromatic Explosives in Surface Water Samples at Ambient Temperature. *Chemosphere* **2009**, *76* (1), 1–8. https://doi.org/10.1016/j.chemosphere.2009.02.050.

(19) Walsh, M. E. Analytical Methods for Detonation Residues of Insensitive Munitions. *J. Energ. Mater.* **2016**, *34* (1), 76–91. https://doi.org/10.1080/07370652.2014.999173.

Table S3. Dissolved TNT concentrations in near-bottom water during cruise AL567. Note that station positions are only reported to two decimal places due to restrictions on reporting munitions-related data.

Station_ID	Date_time	Latitude (deg)	Longitude (deg)	Depth (m)	TNT (ng/L)
AL567_11-1	19/10/2021 11:13	54.48	10.36	19	2.9
AL567_12-1	19/10/2021 11:45	54.47	10.35	15	51.5
AL567_13-4	19/10/2021 13:01	54.47	10.33	15	5.1
AL567_14-4	19/10/2021 13:23	54.47	10.32	17	6.6
AL567_15-2	19/10/2021 13:40	54.47	10.3	19	3.9
AL567_17-2	19/10/2021 14:04	54.48	10.33	19	8.4
AL567_18-2	19/10/2021 14:34	54.49	10.33	20	1.3
AL567_22-1	19/10/2021 18:27	54.46	10.33	13	26.6
AL567_23-1	19/10/2021 18:48	54.46	10.33	12	21.5

AL567_24-1	19/10/2021 19:01	54.46	10.33	11	9.5
AL567_25-1	19/10/2021 19:19	54.46	10.32	8	3.0
AL567_26-1	19/10/2021 19:41	54.46	10.3	11	8.6
AL567_27-1	19/10/2021 20:11	54.46	10.35	11	34.3
AL567_28-1	19/10/2021 20:54	54.47	10.45	15	2.1
AL567_29-1	19/10/2021 21:44	54.39	10.56	14	2.2
AL567_30-1	19/10/2021 22:18	54.38	10.65	12	4.0
AL567_31-1	19/10/2021 22:47	54.39	10.71	18	4.2
AL567_32-1	19/10/2021 23:19	54.42	10.78	12	1.0
AL567_33-1	20/10/2021 00:16	54.5	10.88	12	4.7
AL567_34-1	20/10/2021 01:00	54.56	10.97	13	2.0

AL567_35-1	20/10/2021 01:35	54.59	11.02	23	2.8
AL567_36-1	20/10/2021 02:38	54.57	11.23	29	8.1
AL567_37-1	20/10/2021 03:37	54.49	11.4	28	5.4
AL567_38-1	20/10/2021 04:05	54.46	11.36	19	7.1
AL567_39-1	20/10/2021 04:39	54.39	11.37	22	9.6
AL567_40-1	20/10/2021 05:34	54.32	11.31	21	2.7
AL567_41-1	20/10/2021 06:16	54.25	11.25	21	10.3
AL567_42-1	20/10/2021 06:50	54.2	11.22	20	5.0
AL567_43-1	20/10/2021 07:27	54.14	11.16	22	5.9
AL567_44-1	20/10/2021 08:06	54.12	11.05	15	0.9
AL567_57-1	21/10/2021 11:31	54.05	10.86	21	0.6

AL567_58-1	21/10/2021 12:01	54.07	10.91	22	1.1
AL567_59-1	21/10/2021 12:22	54.08	10.95	22	1.8
AL567_60-1	21/10/2021 12:45	54.11	10.99	22	0.7
AL567_64-1	22/10/2021 09:57	54.09	11.01	22	2.2
AL567_65-2	22/10/2021 10:24	54.07	11.03	22	0.8
AL567_70-1	23/10/2021 09:35	54.07	11.03	23	2.9
AL567_71-1	23/10/2021 10:03	54.05	11.04	24	4.6
AL567_72-1	23/10/2021 10:26	54.05	11	23	1.2
AL567_80-1	23/10/2021 16:48	54.04	10.8	17	4.1
AL567_88-1	24/10/2021 17:42	54.01	10.81	14	2.1
AL567_89-1	24/10/2021 18:30	54.02	10.88	20	1.4

AL567_104-1	25/10/2021 18:28	54.01	10.94	21	4.9
AL567_105-1	25/10/2021 19:35	54.03	10.92	13	1.6
AL567_106-1	25/10/2021 20:22	54.04	10.98	23	5.5
AL567_107-1	25/10/2021 21:02	54.02	11.01	23	2.4
AL567_108-1	25/10/2021 21:54	54.03	11.06	17	6.6
AL567_121-1	26/10/2021 23:25	54.04	11.14	25	3.6
AL567_122-1	27/10/2021 00:09	54.06	11.23	20	4.5
AL567_123-1	27/10/2021 00:56	54.1	11.37	16	5.6
AL567_124-1	27/10/2021 01:38	54.16	11.5	21	2.8
AL567_125-2	27/10/2021 02:31	54.24	11.59	25	2.4
AL567_140-1	27/10/2021 18:15	54.25	11.74	25	3.4

AL567_141-1	27/10/2021 19:21	54.26	11.99	17	3.6
AL567_142-1	27/10/2021 20:03	54.28	12.08	18	3.3
AL567_143-1	27/10/2021 20:51	54.34	12.15	18	1.8
AL567_144-1	27/10/2021 21:23	54.39	12.11	21	4.4
AL567_145-1	27/10/2021 22:07	54.37	11.97	17	1.2
AL567_146-1	27/10/2021 22:56	54.36	11.8	23	4.0
AL567_147-1	27/10/2021 23:57	54.41	11.59	25	2.3
AL567_148-1	28/10/2021 00:41	54.46	11.49	26	2.3
AL567_149-1	28/10/2021 01:50	54.54	11.34	29	2.9
AL567_150-1	28/10/2021 02:48	54.59	11.15	28	3.0
AL567_151-1	28/10/2021 04:02	54.58	10.87	20	1.8

AL567_152-1	28/10/2021 04:36	54.56	10.77	23	1.7
AL567_153-1	28/10/2021 05:09	54.53	10.68	23	3.6
AL567_154-1	28/10/2021 05:41	54.53	10.59	16	1.9
AL567_155-1	28/10/2021 06:18	54.51	10.47	16	4.0
AL567_156-1	28/10/2021 06:59	54.47	10.35	15	4.2
AL567_157-1	28/10/2021 07:12	54.46	10.35	12	5.9
AL567_158-1	28/10/2021 07:26	54.46	10.33	11	5.5
AL567_159-1	28/10/2021 07:43	54.46	10.33	12	2.0
AL567_160-1	28/10/2021 08:05	54.46	10.32	9	15.3
AL567_161-1	28/10/2021 08:21	54.47	10.32	18	35.3
AL567_162-1	28/10/2021 09:06	54.55	10.4	18	2.2

AL567_163-1	28/10/2021 09:38	54.6	10.31	16	1.7
AL567_164-1	28/10/2021 10:18	54.65	10.22	20	2.8
AL567_165-1	28/10/2021 10:52	54.71	10.15	25	1.2
AL567_166-1	28/10/2021 11:33	54.77	10.03	28	2.8
AL567_167-1	28/10/2021 12:07	54.82	9.94	26	2.4
AL567_168-1	28/10/2021 12:48	54.82	9.82	24	1.5